40. EAN
40. MEZINÁRODNÍ KONFERENCE EXPERIMENTÁLNÍ ANALÝZY NAPĚTÍ
40th INTERNATIONAL CONFERENCE EXPERIMENTAL STRESS ANALYSIS
3. – 6. VI. 2002, PRAHA/PRAGUE, CZECH REPUBLIC

STRESS CONCENTRATION IN THE CASE OF CIRCULAR RISER IN THE THIN WALLED TUBE UNDER TENSION AND TORSION

KONCENTRACE NAPĚTÍ U KRUHOVÉHO KONCENTRÁTORU V TENKOSTĚNNÉ TRUBCE NAMÁHANÉ TAHEM A KRUTEM

František Plánička, Vlastimil Vacek, Jaroslav Svoboda*

Abstract: *The influence of the stress concentration caused by notches is of a great importance for the computation both for the static and time – depended loading of components and structures. The contribution is focused on the stress components numerical determination using 3D FEM model and its experimental verification using the electric resistance gauge method.*

Key words: thin walled tube, circular riser, stress concentration, experimental results, numerical modelling

1. Introduction

The paper deals with the stress concentration caused by a circular hole in a thin walled tube subjected to the tension and torsion. The shape and the dimensions of the specimen made from the annealed mild steel ČSN 411523.1 are shown in fig. 1.

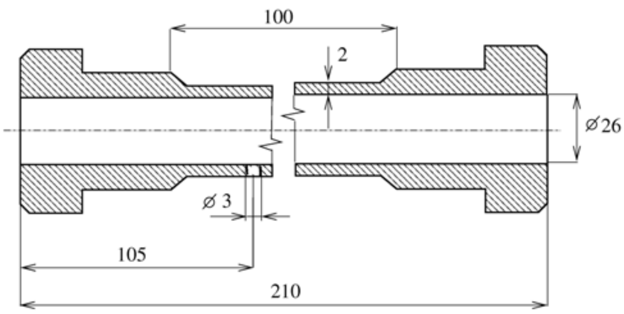

Fig. 1

The chemical composition is presented in table 1.

C [%]	Mn [%]	Si [%]	P [%]	S [%]	N [%]
0.20	1,35	0,38	0,020	0,018	0,008

Tab. 1

*Prof. Ing. František Plánička, CSc., (tel.:019/7491131, fax: 019/7423661, e-mail: planicka@kme.zcu.cz), Ing. Vlastimil Vacek, CSc. , (tel.:019/7491276, fax: 019/7423661, e-mail: vacek@kme.zcu.cz), Department of Mechanics, Faculty of Applied Sciences, University of West Bohemia, Univerzitní 8, 30614 Pilsen, Ing.. Jaroslav Svoboda, Institute of Thermomechanics, Czech Academy of Sciences, Veleslavínova 11, Pilsen,

The thin walled tube was chosen to satisfy the assumption of constant stresses distribution along the tube thickness.

Static mechanical properties of the material are summarised in table 2. Young modulus of elasticity in tension $E = 2{,}185 \cdot 10^5 \ [MPa]$, Poisson ratio $\mu = 0{,}3$.

σ_Y [MPa]	σ_U [MPa]	Ductility A [%]	Area reduction Z [%]
365,1	550,97	32	73

Tab. 2

2. Numerical analysis

The numerical stress analysis was performed by FEM for the 3D – model with the stress riser of diameter $d = 3[mm]$. The spatial model and its loading by the axial force and the torque as well as the coordinate system are obvious from fig. 2. The computational model was created by the MENTAT code and the numerical solution itself was performed by the MARC system.

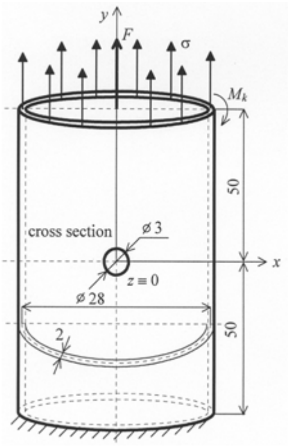

Fig. 2

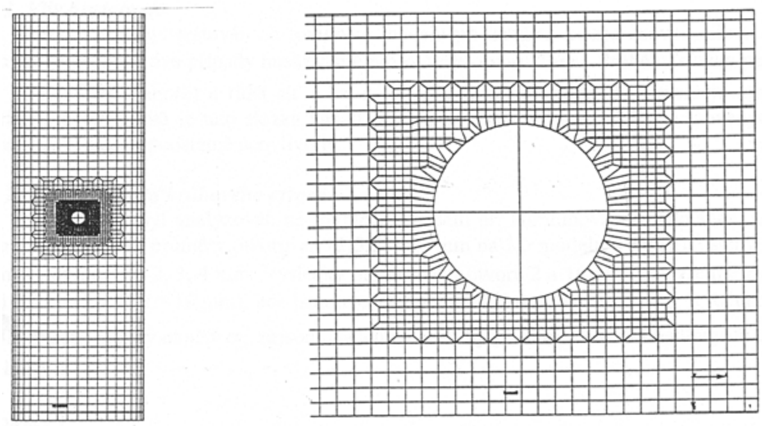

Fig. 3

The model meshing with the detail of the stress riser region zone is shown in fig. 3, number of layers along the thickness was chosen 4. The model was subjected to the normal force and the torque causing normal stress $\sigma = 100[MPa]$ and shear stress $\tau_z = 100[MPa]$.

3. Experimental analysis

For the verification of the normal stress component σ_y caused by the axial force and the resultant shear stress on the specimen surface the electric-resistant strain gauges were used. The location of the gauges at the cross-section is obvious from fig. 4. T_1 is a single gauge LY11-0,6/120, T_2 and T_3 are 3 0º/45º/120º stacked rosettes RY91-1,5/120 from HBM, Ltd. The gauge T_1 was used for the normal stress component σ_y measurement, the gauge T_2 mode gives possibility to determine both the normal stress component σ_y and the shear stress component in the region of their extreme. The location of the gauge T_2 was determined as a compromise between the numerical results and the gauge dimensions. The gauge T_3 was used as a control one, because it is located in the place, which is not influenced by the stress concentration.

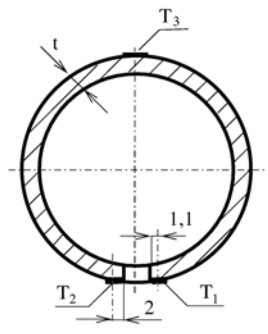

Fig. 4

The measurement itself was realised by the measuring system UGR 60, HBM Ltd. The specimen was loaded in the electro-hydraulic testing machine INOVA YUY 200-1 with computer controlled functions.

4. Stress analysis

The diagram in fig. 5 presents the resultant shear stress as a function of the wall thickness at the place of the maximum shear stress and at the shifted section (90º, 180º, 270º) for the specimen loading corresponding to the shear stress $\tau_z = 100[MPa]$. The nominal shear stress in minimum cross-section for this loading is $\tau_n = 103{,}5[MPa]$. It is obvious from the diagram, that even for the case of a thin wall tube the shear stress changes along the thickness. In the locus of its maximum the change is non-linear and the difference between the values at the inner and outer surfaces is about 13%. The maximum value $\tau = 155{,}3[MPa]$ corresponds very well to the experimentally determined value 149,5 [*MP*] – see also the diagram in fig. 6.

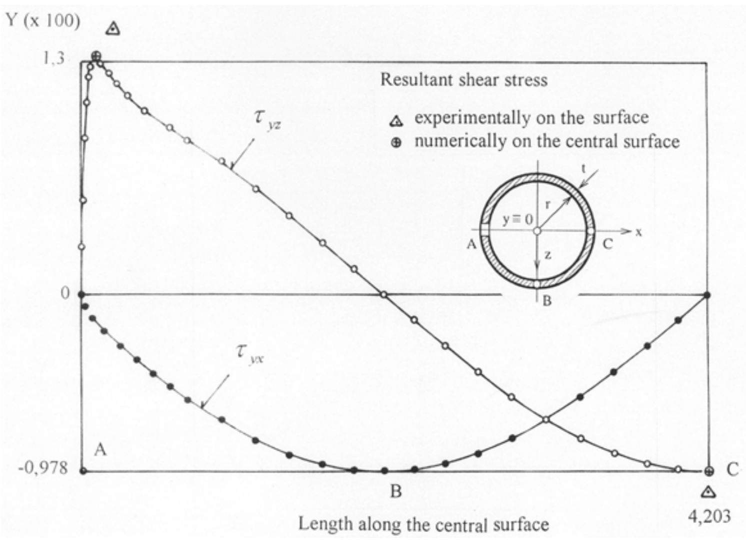

Fig. 5 Fig. 6

In the sections shifted by the angle 90º, 180º and 270º the change of the shear stress is linear and the difference between the inner and outer surfaces is about 14 ÷ 18%. In the sections shifted by 90º and 270º the stress values are the same. As it is obvious from the diagram, the experimentally determined value at the 180º section is between the values for 90º and 270º.

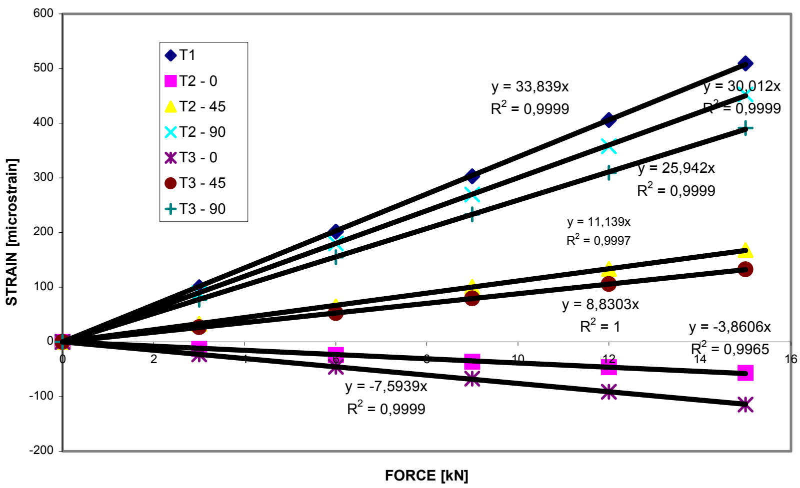

Fig. 7

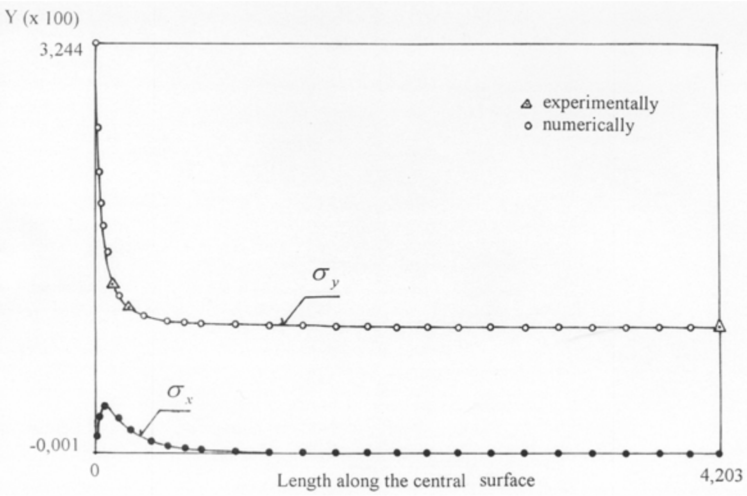

Fig.8

In fig. 6 the course of shear stress components τ_{yz} and τ_{yx} along the central cylindrical surface is presented. For the comparison the experimentally determined values on the specimen outer surface (as they are presented in fig. 5) are shown in fig. 6.

In fig. 7 the values of strains obtained from the single gauge T_1 and from the rosettes T_2 and T_3 as functions of loading are presented. The high accuracy of the measurement with nearly zero deviations from the mean values is obvious from this diagram. In fig. 8 the stress components σ_x, σ_y are shown for the loading $\sigma = 100[MPa]$, to which the nominal stress $\sigma_n = 103{,}5[MPa]$ at the minimal cross-section corresponds. In this figure the experimentally obtained values of the stress component σ_y for the same loading are presented. It can be concluded that the agreement between the numerical solution and the experiment is very good.

5. Stress concentration factor determination

On the basis of the above obtained results it is possible to compute corresponding stress concentration factors for the tube with a circular stress riser subjected to the tensile and torsion.

Than, for the tension we obtain $\alpha_\sigma = \frac{(\sigma_y)_{\max}}{\sigma_n} = 3{,}1$ and for the torsion $\alpha_\tau = \frac{\tau_{\max}}{\tau_n} = 1{,}44$.

6. Conclusion

Components with different stress risers statically and dynamically loaded are communally used. At present strain and stress fields are usually determined numerically using FEM. The question is whether, especially for the stress risers of small dimensions, the used method can describe the stress concentration with sufficient accuracy. The authors´ aim was to contribute to the answer to the above question. It is obvious from the presented results, that for the case of the tensile loading the sufficient agreement with published results was obtained for adequate fine meshing.

However for the case of the torsion the value of the stress concentration factor was significantly lower than that in literature, where for the thin-walled tube with two opposed circular holes the stress concentration factor is $\alpha > 3{,}5$. In spite of the nearly the same results of the numerical solution and the experiment, this problem will have to be further studied.

This research was supported by the research project MSM 235200003.

References:

[1] Hertel, H.: Ermüdungstestigkeit der Konstruktionen, Springer – Verlag, Berlin, Heidelberg, New York 1969.
[2] Peterson, P.: Koefficienty koncentracii naprjazenij, Izdatelstvo Mir, Moskva, 1977.
[3] Plánička, F. – Bojčuk, L.: Numerical stress state analysis in a thin-walled tube a stress riser, Proceedings of 16th Conference of Computational Mechanics 2000, Nečtiny (in Czech).